Int. J. Environ. Sci. Technol. (2016) 13:529–542
DOI 10.1007/s13762-015-0857-3

ORIGINAL PAPER

Biodegradation of phenol by a novel diatom BD1IITG-kinetics and biochemical studies

B. Das[1] · T. K. Mandal[2] · S. Patra[3]

Received: 14 January 2015 / Revised: 17 April 2015 / Accepted: 7 July 2015 / Published online: 30 July 2015

Abstract A phenol-degrading novel diatom BD1IITG was isolated from petroleum refinery wastewater and characterized (GenBank Accession No. KJOO2533). HPLC analysis showed the diatom could degrade phenol in the concentration range of 50–250 mg/l in Fog's media. The highest specific growth and degradation rate were achieved at 100 mg/l phenol. It could also mineralize phenol along with aliphatics in petroleum refinery wastewater. Growth kinetic modeling shows that Haldane model best represents the growth behavior of the diatom in nutrient media as well as refinery wastewater. Biokinetic parameters suggest that the diatom possesses higher maximum specific growth rate ($\mu_{max} = 0.4$ day^{-1}), better tolerance to toxicity ($K_I = 90.24$ mg/l) and high phenol affinity ($K_s = 20.99$ mg/l) in refinery wastewater as compared to Fog's media confirming practical applicability of the strain for wastewater treatment. FTIR fingerprinting of biomass indicates intercellular phenol uptake and breakdown into its intermediates via phenol degradation pathway. Pathway was elucidated using HPLC, LC–MS and UV–visible spectrophotometry confirming prominence of ortho- over meta pathway for phenol metabolism. The diatom produces biosurfactant with highest emulsifying activity at 100 mg/l phenol which may contribute to highest degradation rate at this concentration. Infrared analysis confirms increased biosynthesis of lipids and polysaccharides in phenol-degrading biomass, indicating its potential use as feedstock of clean ecofriendly energy sources as biodiesel or bioethanol. The phenol degradation capability coupled with potential applicability of the spent biomass as biofuel feedstock makes diatom BD1IITG a potential candidate for a clean environmentally sustainable process.

Graphical Abstract

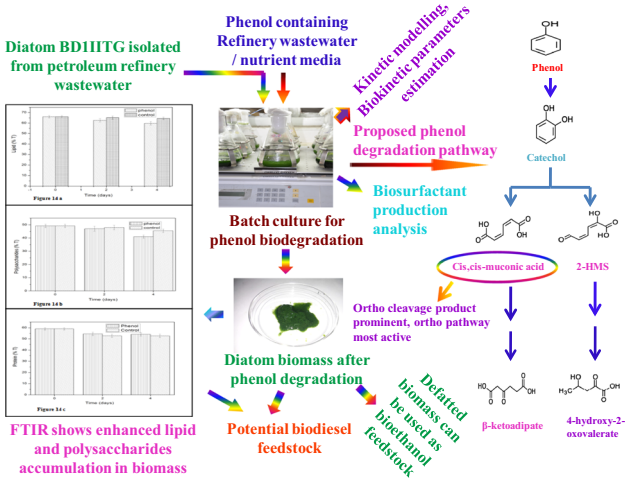

Keywords Phenol · Diatom · Biodegradation · Growth kinetics · Pathway · Biosurfactant · Biofuel

Electronic supplementary material The online version of this article (doi:10.1007/s13762-015-0857-3) contains supplementary material, which is available to authorized users.

✉ S. Patra
sanjukta@iitg.ernet.in

[1] Centre for the Environment, Indian Institute of Technology Guwahati, Guwahati, Assam, India

[2] Department of Chemical Engineering, Indian Institute of Technology Guwahati, Guwahati, Assam, India

[3] Department of Biotechnology, Indian Institute of Technology Guwahati, Guwahati 781039, Assam, India

Introduction

Phenol produced annually at around 7 billion kg is used as a raw material in various industries such as oil refining, pharmaceuticals, pesticides, coking plants as well as leather industries (Senthivelan et al. 2014). Phenol is released in the wastewaters of these industrial processes. Due to high water solubility of phenol (8.3 g/100 ml), it easily reaches downstream water sources from discharges causing harmful effects to aquatic flora, fauna and humans. Phenol is responsible for causing severe biochemical oxygen demand (BOD) which affects the aquatic organisms. Long disposal of phenol on land causes negative effect on fertility of the land (Senthivelan et al. 2014). Owing to the toxic nature of phenol, it is placed under priority list of pollutants that need to be treated before releasing the wastewater to the aquatic ecosystems. The total phenol in refinery wastewater has been estimated to be 13–88 mg/l (Abdelwahab et al. 2009; Jou and Huang 2003; Ojumu et al. 2005; El Naas et al. 2010). Conventional phenol removal techniques include solvent extraction, adsorption, coagulation and chemical oxidation. However, most of these techniques yield secondary by-products which incur additional costs for treatment (Senthivelan et al. 2014). Biological degradation owing to its advantages of complete mineralization of organic pollutants as well as low costs has gained wide attention for treatment of effluents. Biological treatment of phenol-containing wastes faces challenge of substrate inhibition where cell growth as well as concomitant degradation is hindered by toxicity of phenol (Senthivelan et al. 2014). Phenol-polluted wastewater and soil are main sources of phenol-degrading microbial strains (bacteria, fungi and algae). Algal phenol degradation capability is much less studied as compared to bacterial and fungal strains. Phenol biodegradation ability has been reported by strains of *Chlorella* sp., *Scenedesmus obliqus* and *Spirulina maxima* (Kelknar and Kosarnic 1992), *Ochromonas danica* (Semple and Cain 1996), *Ankistrodesmus braunii* and *Scenedesmus quadricauda* (Pinto et al. 2003), *Chlorella vulgaris* (Scragg 2006; El-Sheekh et al. 2012), *Chlorella VT-1* (Scragg 2006), *Volvox aureus*, *Lyngba lagerlerimi*, *Nostoc linkia*, *Oscillatoria rubescens* (El-Sheekh et al. 2012). Reports are available only on phenol degradation ability by microalgae with no further details of kinetics and enzymatic pathway of phenol metabolism. However, among diatom (a major group of algae), only one marine diatom *Thalassiosira* sp. has been reported to have phenol degradation ability (Lovell et al. 2002). The present study reports for the first time isolation of a phenol-degrading diatom from petroleum refinery wastewater. Microbial phenol degradation is a strong function of biomass growth; the knowledge of growth kinetics is valuable information leading to understanding the capacity of the microbe for phenol degradation. Keeping the necessity to evaluate growth kinetics in mind, growth inhibitory models to describe the microbial growth dynamics in the presence of growth inhibitory substrate as phenol have been proposed (Banerjee and Ghoshal 2010). Biokinetic parameters obtained from the growth kinetic model best fitting to the experimental data are a necessary input for design of biological remediation processes with optimized operational conditions for treatment of phenol-polluted wastewater (Sahoo et al. 2011; Banerjee and Ghoshal 2010). In a bid to verify the practical applicability of the diatom, the kinetics underlying phenol degradation by the diatom in petroleum refinery wastewater was studied. The enzymatic mechanism behind the phenol-degrading capability of the diatom species was elucidated which is the first proposed enzymatic pathway for phenol degradation in any diatom species. The present study reports for the first time biosurfactant-mediated facilitation of microalgal phenol degradation process. To identify any potential application of the spent biomass as feedstock of ecofriendly clean energy sources as biodiesel and bioethanol, the biochemical quality of the phenol-degrading biomass was analyzed.

Materials and methods

Chemicals

$MgSO_4$, $CaCl_2$, K_2HPO_4, $FeSO_4$, Na_2EDTA, H_3BO_3, $MnCl_2{\cdot}4H_2O$, $ZnSO_4{\cdot}7H_2O$, $Na_2MoO_4{\cdot}2H_2O$, $CuSO_4{\cdot}5H_2O$ and phenol were of analytical grade obtained from Merck, India. Catechol and *cis*,*cis*-muconic acid standards were of high-performance liquid chromatography (HPLC) grade obtained from Sigma-Aldrich, India. Fourier transform infrared spectroscopy (FTIR)-grade KBr was obtained from Spectrochem, India.

Isolation and molecular identification of phenol-tolerant diatom strain

Wastewater algal species was cultured in Fog's media containing 20 mg/l phenol and 5 g/l ampicillin to avoid any bacterial contamination in culture (Joo and Lee 2007). The alga was cultured at an illumination of 3500 lux, photoperiod of 14 h light: 10 h dark and 140 rpm. The culture was purified by subsequent transfer to 20 mg/l phenol-supplemented media with ampicillin. 16S ribosomal RNA (16S rRNA) gene sequencing of the phenol-tolerant strain was carried out at M/s Qubebioscience private Limited, Hyderabad, India, and the sequence was

submitted to National Centre for Biotechnology Information (NCBI) GenBank, and an accession number was obtained. The gene sequence homology was analyzed using Basic Local Search Alignment (BLAST) tool of NCBI, USA, and phylogenetic tree was constructed using robust phylogenetic analysis for the non-specialist (Deereeper et al. 2008).

Biomass growth, phenol degradation and growth kinetic modeling analysis

The phenol degradation ability of the diatom was analyzed in the phenol concentration range of 50–250 mg/l. The biomass growth was analyzed at equal intervals of 24 h by carrying out dry weight analysis. The residual phenol at equal intervals of 24 h was analyzed by HPLC with UV–visible detector operating at 270 nm in a C-18 column with mobile phase of acetonitrile–water (70:30) at flow rate of 0.5 ml/min. To determine loss of phenol due to abiotic factors, phenol media without inoculation of diatom were incubated in same condition followed by dry weight analysis and residual phenol analysis by HPLC. The specific growth rate (μ) at different phenol concentrations was determined by fitting a linear function to exponential phase of ln $x(t)$ versus time curve, where $x =$ biomass (mg/l) and $t =$ time (days) (Baranyi 2010). The experimental data were analyzed with several available growth kinetic models like Haldane (Haldane 1965), Yano (Yano et al. 1966), Webb (Webb 1963), Aiba (Aiba et al. 1968), Edward (Edwards 2004) to select a suitable kinetic model that can represent growth pattern of *C. pyrenoidosa* in the presence of phenol. From the experimental data of specific growth rate (μ, day^{-1}) at various initial concentration of phenol (S_0), the model equations were solved using nonlinear regression method (Excel, Microsoft office) and the values of kinetic parameters of different models were determined based on highest regression coefficient (R^2) and least standard deviation (SD) value (Saravanan et al. 2008; Duan 2011; Hasan and Jabeen 2015). The specific degradation rate was determined from the gradient of a semi-logarithmic plot of substrate concentration, S, versus time for each initial phenol concentration under study (S_0) (Banerjee and Ghoshal 2010).

In order to analyze the practical applicability of the isolated diatom, the growth and phenol degradation kinetics was studied in petroleum refinery wastewater. Wastewater from an Indian petroleum refinery was collected and stored at 4 °C for further analysis. The analysis of the oil components in refinery wastewater was carried out by China National Standard Method (Zhao et al. 2006). The amount of phenol in refinery wastewater was analyzed by HPLC as mentioned above. The isolated diatom was inoculated to petroleum refinery wastewater to verify its phenol degradation efficiency in real wastewater. The biomass growth as well as phenol degradation in refinery wastewater was characterized at regular intervals of 24 h using dry weight analysis and HPLC, respectively. The specific growth and degradation rates were estimated by fitting the experimental growth kinetic data to the growth kinetic models. Following treatment of the wastewater with the diatom, changes in other oil components of refinery wastewater were characterized by China National Standard Method (Zhao et al. 2006).

FTIR fingerprinting of phenol-degraded biomass

FTIR analysis of phenol-degraded biomass was performed with two objectives: (a) To determine whether phenol is biodegraded or bioaccumulated in the cell and (b) to analyze the biochemical changes in the algal biomass during the phenol removal process. Actively phenol-utilizing algal cells (100 mg/l phenol) were harvested and dried in vacuum desiccators. One volume of dried biomass was blended with 100 volume of dried KBr powder and pressed into tablets before FTIR measurement. The spectral acquisition was carried out in FTIR spectrometer (Perkin Elmer, USA) by means of 500 scans with 4 cm^{-1} of spectral resolution over the wave number range of 400–4000 cm^{-1}.

Characterization of the phenol degradation pathway

Enzyme induction in algal biomass was carried out in 100 mg/l phenol-supplemented Fog's media since specific growth and degradation rate were highest at this concentration. Actively phenol-degrading biomass was harvested by centrifugation (3000 rpm, 10 min, 4 °C), washed with 50 mM potassium phosphate buffer and ground in a mortar. The extract was centrifuged (10,000 rpm, 10 min, 4 °C), and the supernatant obtained was used for enzyme activity assays. Total protein in the supernatant was determined by Lowry protein assay. Phenol hydroxylase activity was determined in an assay mixture of potassium phosphate buffer (pH 7.2), crude enzyme extract, phenol and NADPH. Control incubation was carried out using heat-inactivated enzyme extract. Phenol utilization and concomitant accumulation of the reaction product catechol were monitored by HPLC. The ortho cleavage of catechol (hydroxylation product of phenol) to *cis*,*cis*-muconic acid was carried out by catechol-1,2-dioxygenase. Catechol-1,2-dioxygenase activity was studied in an assay mixture containing 50 mM potassium phosphate buffer, pH 7.2, protein and catechol. Ortho cleavage of catechol to *cis*,*cis*-muconic acid was analyzed by HPLC. Catechol-2,3-dioxygenase causes meta cleavage of catechol to 2-hydroxymuconic

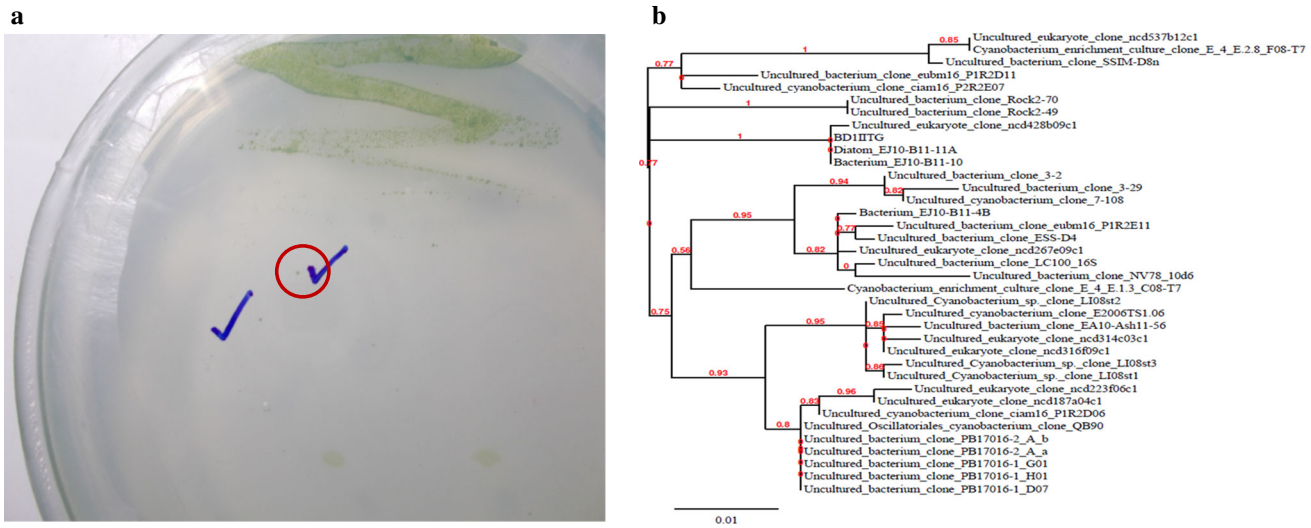

Fig. 1 **a** Single colony of diatom BD1IITG (colony marked by *red circle*) isolated by streak plate method, **b** phylogenetic tree constructed using robust phylogenetic tree for the non-specialist

semialdehyde (2-HMS). The reaction conditions were same as in catechol-1,2-dioxygenase assay. Catechol-2,3-dioxygenase activity was analyzed by increase in absorbance at 375 nm due to accumulation of the meta cleavage product 2-HMS (E_{375} = 14,700 mol/l/cm) by UV–visible spectrophotometry.

The further metabolites produced by breakdown of *cis*,*cis*-muconic acid and 2-HMS were identified by electrospray ionization liquid chromatography–mass spectrometry (LC–MS) (Infinity LC system, Agilent, USA) in positive charge mode. For LC–MS analysis, acetonitrile/water (60:40) mixture was used as solvent at a flow rate of 0.5 ml/min with detector operating at 270 nm. The mass-to-charge ratio (*m*/*z*) signals were identified using the Tandem Mass Spectrum database (open source: Central Drug Research Institute, India).

Analysis of biosurfactant production

Many microbial species produce biosurfactant which changes the solubility and dispersion of hydrocarbons, thus increasing its availability to the microbial cells. Biosurfactant induces rise in cell surface hydrophobicity which changes the affinity between microbial cell and hydrocarbon, thus leading to increased biodegradation rates (Hassan et al. 2014). The biosurfactant production ability was analyzed by the emulsification assay as per Rocha et al. (2007). In this assay, 2 ml of culture was vortex mixed with same volume of kerosene and left to stand for 24 h. The emulsification index (E 24) was calculated as percentage of the height of the emulsified layer (mm) divided by height of the liquid column (mm).

Statistical analysis

All experiments were carried in triplicates, and the mean values and standard error were calculated using Origin Pro8 (Origin Lab Corporation, Northampton, MA, USA) and reported in the respective plots.

Results and discussion

Isolation and molecular identification of phenol-tolerant diatom

Phenol-tolerant single algal colonies were isolated from refinery wastewater (Fig. 1a). The isolate BD1IITG (Fig. 1a, single colony marked in red circle) was identified on basis of 16S rRNA plastid gene sequence. BLAST analysis suggests the isolate BD1IITG to be a diatom based on homology with 99 % identity to 16S rRNA plastid sequence of diatom EJ10-B11-11A. The high bootstrap support of the phylogenetic tree (Fig. 1b) demonstrated that the isolate BD1IITG belongs to the algal group diatom owing to close evolutionary relationship with diatom EJ10-B11-11A. The 16S rRNA gene sequence of diatom BD1IITG was deposited to NCBI GenBank, and an Accession No. KJOO2533 was obtained.

Biomass growth, phenol degradation and growth kinetic modeling

The effect of initial phenol concentration on biomass growth profile and phenol degradation by diatom BD1IITG

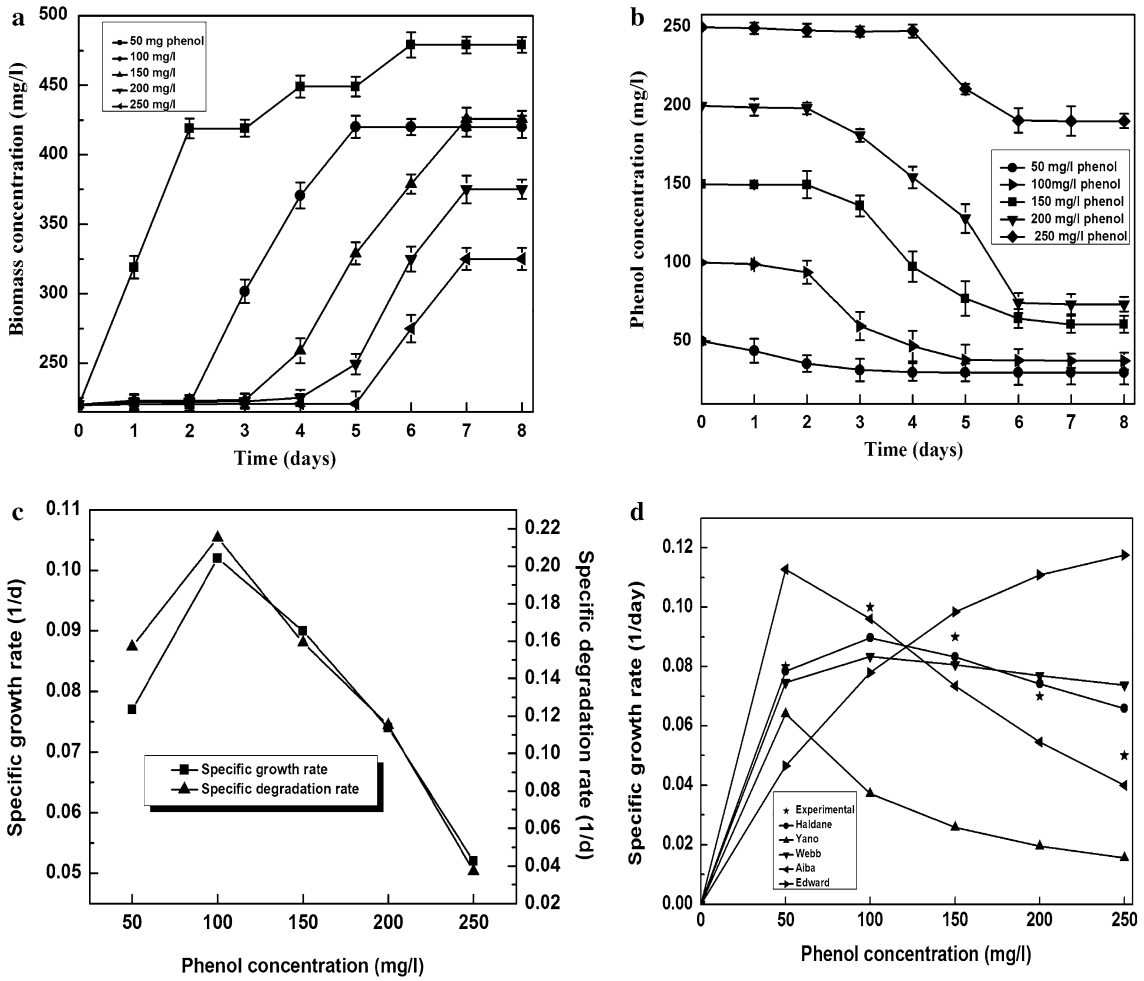

Fig. 2 **a** Biomass growth profile of diatom BD1IITG, **b** phenol degradation profile of diatom BD1IITG, **c** specific growth and degradation rate for various concentrations of phenol, **d** experimental and growth kinetic model predicted specific growth rates

has been shown in Fig. 2a, b. The growth curve shows that there is no lag phase at 50 mg/l phenol culture. A lag phase in the biomass growth profile is evident at 100 mg/l phenol and the phenol concentrations thereafter. Lag phase is followed by exponential biomass growth which is associated with phenol utilization by the biomass. The algal cells then finally enter into stationary phase where there is no more phenol utilization. Li et al. (2010) reported association of lag periods with increased initial phenol concentration and phenol degradation in the exponential growth phase which corroborates with the present findings. The specific growth rate increased with increase in phenol concentration until highest growth rate of 0.102 day^{-1} was achieved at phenol concentration of 100 mg/l (Fig. 2c). With increase in phenol concentration beyond 100 mg/l, the growth rate declines indicating growth inhibition effect of phenol.

The phenol degradation profile was determined by HPLC with a retention time of 19.4 min. Figure 2b clearly indicates that the diatom degrades 39.88 % (for 50 mg/l phenol), 63 % (for 100 mg/l phenol), 59.52 % (for 150 mg/l phenol), 51.23 % (for 200 mg/l phenol) and 24 % (for 250 mg/l phenol). The specific degradation rate increases with increase in phenol concentration until maximum degradation rate of 0.215 day^{-1} was achieved at 100 mg/l phenol (Fig. 2c). It is due to the highest specific growth rate of the microalgae at 100 mg/l phenol. This reflects phenol degradation to be a growth-dependent phenomenon. Beyond 100 mg/l phenol concentration, progressive decrease in specific degradation rate could be well explained by inhibited biomass growth. Mathur and Majumder (2010) studied phenol degradation by *Pseudomonas putida* and observed a similar phenomenon of increased specific growth and degradation rate with increase in substrate concentration until a maximum phenol concentration of 100 mg/l. They also reported that both growth and degradation rate decline due to substrate inhibition of phenol concentration >100 mg/l which accords

with findings of present study. About 1 % abiotic loss of phenol was found within 5 days as compared to 63 % phenol removal in 100 mg/l phenol cultures. This proves that the diatom is solely responsible for phenol removal from the sample. Microbial biodegradation rate is dependent on biomass growth rate. A higher biomass growth rate results in increased biodegradation rate (Agarry et al. 2008). Thus, evaluation of microbial growth kinetics will bring forward its potential for biodegradation of organic compounds. An attempt has been made to find out the mathematical relationship between biomass growth rate and substrate concentration. For this, the biokinetic parameters were estimated using the various substrate inhibitory models. The parameters obtained by solving the various growth kinetic models have been tabulated in Table 1. From this table, it is clear that Haldane model yielded comparatively high R^2 value and least SD value confirming that experimental data best fitted into the Haldane model. Figure 2d shows a comparative plot of experimentally observed variation in specific growth rate of diatom BD1IITG at different initial phenol concentrations as well as the prediction of the experimental data by five different growth kinetic models.

Attempts were also made to analyze the dynamics of biomass growth and phenol degradation of diatom BD1IITG in refinery wastewater. The refinery wastewater was estimated to contain 23.33 mg/l phenol by HPLC. Intending to understand the natural growth and phenol degradation profile of the diatom, the refinery wastewater experiment was carried out without supplementing with any media or media component. Figure 3a shows the growth and phenol degradation ability of the diatom in refinery wastewater. The biomass growth undergoes a lag phase of 2 days unlike absence of lag phase even at 50 mg/l phenol in Fog's media. After the lag phase, there is exponential biomass growth to fourth day and then the biomass enters the stationary phase of growth on fifth day with a final biomass of 493.66 mg/l. The specific growth rate of biomass in refinery wastewater is 0.17 day^{-1}. There is only 2.36 % phenol removal by diatom when it is in the lag phase of growth (till second day). After second day, the algal phenol uptake rate increases which is coincident with exponential biomass growth. Diatom BD1IITG mineralized 68.58 % of phenol in refinery wastewater. The specific degradation rate of phenol by diatom BD1IITG in refinery wastewater was 0.23 day^{-1}. Analysis of the nature of oil in refinery wastewater by UV spectrophotometry shown in Fig. 5 indicates that the refinery wastewater (Fig. 3b, Day 0, solid line) consists of both alkane (absorbance at 215–230 nm) and aromatic compounds (absorbance at 250–260 nm). Since the high absorbance is observed around 215–230 nm, the nature of oil in refinery wastewater is clean oil. Both alkane and aromatic compounds in refinery wastewater were found to be degraded after treatment with diatom BD1IITG for 6 days (dotted line, Fig. 3b). The degradation ability of alkane adds to potential of the diatom strain for bioremediation application. Growth kinetic modeling of diatom BD1IITG in refinery wastewater was also carried out to verify the applicability of diatom BD1IITG for phenol removal from actual refinery wastewater. Table 2 shows the kinetic parameters obtained for various growth kinetic models. Table 2 indicates that Haldane model yielded the highest correlation coefficient (R^2) and the least standard deviation (SD) and thus best fitted the experimental data. Thus, Haldane model best represents the growth behavior of the diatom in refinery wastewater.

Biokinetic parameters comparison could help understand the biomass growth behavior of the diatom under two significantly different culture conditions of nutrient sufficient media and refinery wastewater. For this, the respective biokinetic parameters of best fit kinetic models representing the biomass growth behavior in both the culture conditions were analyzed. The value of K_s (half-saturation coefficient) shows the affinity of the microorganism to the substrate. K_s being inversely related to affinity of microbial system for substrate, a higher K_s value indicates its lower affinity to the substrate (Firozjaee et al. 2011). The value of K_I (substrate inhibition constant) denotes the resistance of microorganism to the toxic effect of the substrate (Sahoo et al. 2011). Kinetic modeling of the experimental biomass growth data indicates that μ_{max} (0.4 day^{-1}) and K_I (90.24 mg/l) are higher in refinery wastewater (first row in Table 2) as compared to that in nutrient media (first row in Table 1). The K_s value (20.99 mg/l) in refinery wastewater (first row in Table 2) is lower than that in nutrient media (first row in Table 1). A similar study was carried out for degradation of phenol in

Table 1 Estimated value of growth kinetic parameters of diatom BD1IITG in phenol-containing nutrient media

Model	μ_{max} (day^{-1})	K_s (mg/l)	K_I (mg/l)	K (mg/l)	R^2	SD
Haldane	0.3	109.99	80.24	–	0.94	0.008
Yano	0.22	2.6	21.5	2000.54	0.67	0.043
Webb	0.27	107.93	30.9	156.06	0.84	0.013
Aiba	0.23	23.13	150.4	–	0.44	0.102
Edward	0.25	170	700.9	–	0.35	0.204

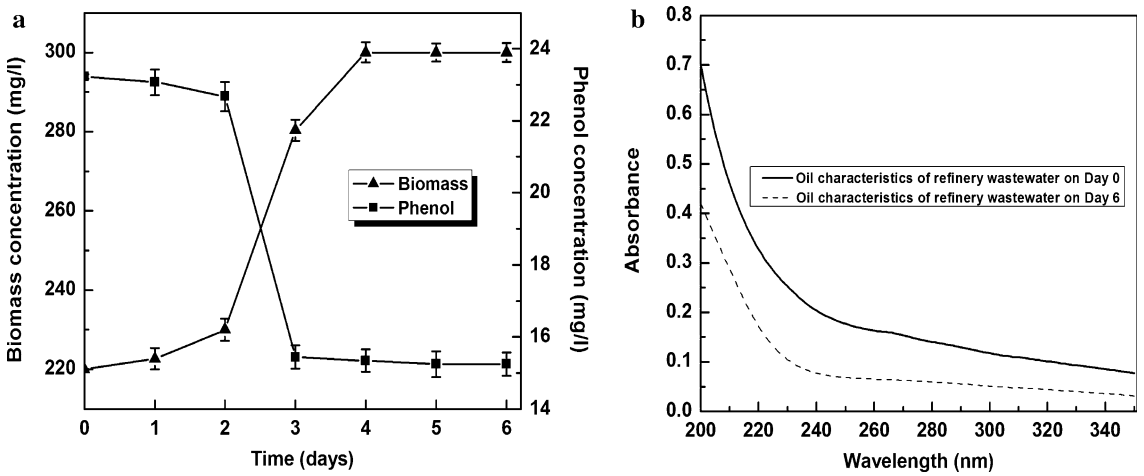

Fig. 3 **a** Biomass growth as well as phenol degradation of diatom BD1IITG in refinery wastewater, **b** characterization of oil components in refinery wastewater before (Day 0) and after (Day 6) treatment with diatom BD1IITG

Table 2 Estimated value of growth kinetic parameters of diatom BD1IITG in refinery wastewater

Model	μ_{max} (day^{-1})	K_s (mg/l)	K_I (mg/l)	K (mg/l)	R^2	SD
Haldane	0.4	20.99	90.24	–	0.99	0.002
Yano	0.17	120.6	100.6	450.54	0.28	0.6
Webb	0.1	170.93	50.9	1500.06	0.88	0.11
Aiba	0.23	678.5	5.3	–	0.46	0.45
Edward	0.23	5.94	105.9	–	0.97	0.009

refinery wastewater (30 mg/l) by two bacterial strains *Pseudomonas aeruginosa* and *Pseudomonas fluorescence* (Agarry et al. 2008). The K_I value (90.24 mg/l) obtained in present study is higher than the K_I value obtained for *Pseudomonas aeruginosa* (29.7 mg/l) and *Pseudomonas fluorescence* (31.7 mg/l). In contrary to present study, Agarry et al. (2008) added nutrient medium to refinery wastewater to maintain the nutritional requirements for biomass growth. The biokinetic parameters suggest that diatom BD1IITG could prove to be an efficient strain for phenol removal from refinery wastewater due to the following characteristics: (a) High μ_{max} (0.4 day^{-1}) value obtained (in refinery wastewater) indicates potential of the diatom for efficient biomass growth in refinery wastewater. (b) Lower K_s value (20.99 mg/l) suggests that the diatom has good affinity for phenol in refinery wastewater which would be beneficial in better phenol uptake rates. (c) High K_I value (90.24 mg/l) indicates better tolerance to toxic effect of substrate in refinery waste water. The increased growth rate as well as phenol uptake efficiency of the diatom BD1IITG in refinery wastewater could be related to nature of the refinery wastewater used in the present study. Cometabolism of alkanes present in the wastewater along with phenol (aromatic) as discussed above (Fig. 3a, b) could have positive effect on biomass growth as well as phenol degradation rates. Sun et al. (2012) studied the cometabolism of aromatic phenol and petroleum alkane in *Acinetobacter* strains and reported enhancement in both biomass growth and phenol degradation rate. Cometabolism of alkanes as well as phenol could provide two parallel carbon sources for the cell which results in more carbon available for cell growth (Sun et al. 2012). An increased biomass growth rate could lead to better phenol degradation rates.

Determination of biodegradation or bioaccumulation of phenol in algal cells

To determine intracellular phenol accumulation and its breakdown to intermediate products (biodegradation) or phenol accumulation in the cells (bioaccumulation), infrared analysis (Fig. 4) of the biomass was carried out. Adsorption at 3444–3419 cm^{-1} was due to stretching of OH groups of alcohol, phenol or carboxyl OH (Droussi et al. 2009). Infrared spectrum shows that the % transmittance in this region decreases with phenol incubation unlike that in control cells (Fig. 4a). Decreased % transmittance indicates increased intracellular phenol accumulation in biomass which is concomitant with increased phenol removal from the medium with incubation time. Catechol is the first intermediate of phenol biodegradation pathway. The products downstream of catechol contains

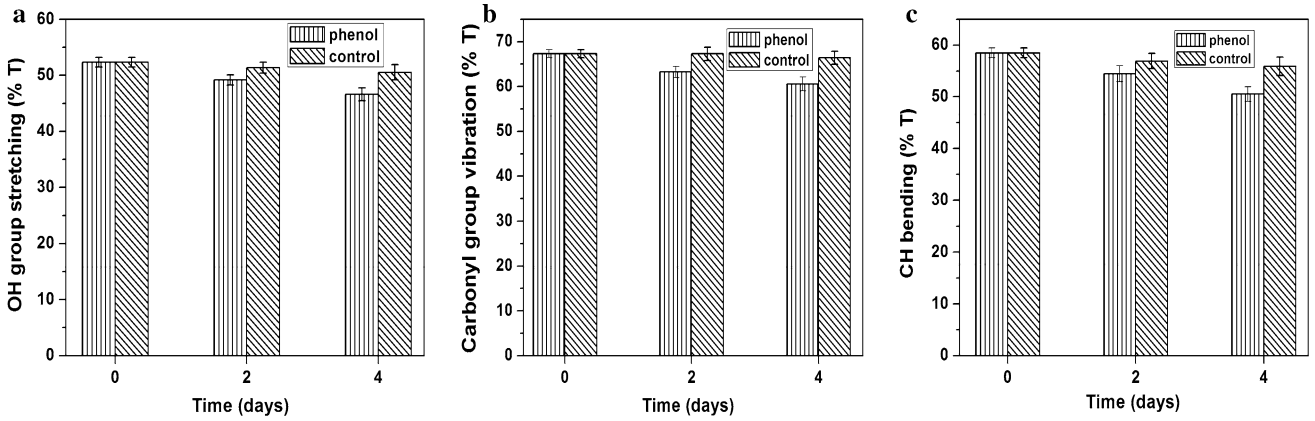

Fig. 4 **a** Change in FTIR peak area corresponding to OH group stretching (of the type of phenol) with incubation time, **b** change in FTIR peak area associated with carbonyl group vibration (of COOH group) with incubation time, **c** change in FTIR peak area attributed to CH bending (of aliphatic groups) with incubation time

carboxylic acid group (–COOH). The infrared spectra region 1754–1710 cm^{-1} are associated with carbonyl group vibration in COOH group (Wharfe et al. 2010). Transmittance in this area was found to decrease with phenol incubation unlike in control cells (Fig. 4b). This shows that the accumulated intercellular phenol is broken down to intermediate products downstream of catechol. Wharfe et al. (2010) also reported similar increased absorbance due to carbonyl group vibration of intermediate breakdown products of phenol in a microbial consortium. The infrared region 1440–1380 cm^{-1} is attributed to CH bending of aliphatic groups. Decreased % transmittance in this wavenumber range indicates increased accumulation of aliphatics in phenol-incubated cells (Fig. 4c). Aliphatic intermediates of phenol metabolism may possibly lead to decreased transmittance. Thus, infrared analysis suggests intracellular uptake of phenol by diatom BD1IITG. The intracellular accumulated phenol is broken into further metabolites confirming the process of phenol removal to be biodegradation.

Elucidation of phenol degradation pathway

The phenol metabolic pathway was elucidated by identifying the different intermediates produced during phenol degradation by using HPLC, UV–visible spectrophotometry and LC–MS. Analysis of phenol-degrading culture media by HPLC (Supplementary Fig. 1a, b) confirms the accumulation of catechol (retention time 10.9 min), the first intermediate of phenol degradation pathway. El-Sheekh et al. (2012) reported similar observation of catechol accumulation in culture media during phenol degradation by algal species as *Volvox aureus*, *Nostoc linkia*, *Oscillatoria rubescens*. Catechol accumulation in culture media confirms that phenol is degraded through an enzymatic pathway in the diatom BD1IITG. Intercellular phenol hydroxylase activity was determined by HPLC (Fig. 5a). Phenol hydroxylase was found to hydroxylate phenol to its reaction product catechol. Control incubations were carried out by heat-killed enzyme extract showing no phenol hydroxylation activity (no phenol utilization and no catechol production). Similar observations have also been reported for algae (Semple and Cain 1996), fungi (Neujhar and Gaal 1973; Páca et al. 2007) and bacteria (Mahiuddin et al. 2012; Ali et al. 1998). Catechol can be ortho cleaved (if it follows ortho pathway) or meta cleaved (if it follows meta pathway) by catechol-1,2-dioxygenase and catechol-2,3-dioxygenase, respectively. Catechol-1,2-dioxygenase activity was determined by identifying its ortho cleavage product, namely *cis*,*cis*-muconic acid (retention time: 4.2 min) using HPLC (Fig. 5b). No catechol-1,2-dioxygenase activity was observed in control incubations carried out by heat-killed enzyme extract. Catechol-2,3-dioxygenase activity was determined by identifying 2-hydroxymuconic semialdehyde as the meta cleavage product of catechol using UV–visible spectrophotometry (Fig. 5c). Control incubations by heat-killed enzyme extract showed no accumulation of meta cleavage product 2-hydroxymuconic semialdehyde indicating no catechol-2,3-dioxygenase activity. Both catechol-1,2-dioxygenase and catechol-2,3-dioxygenase activity suggested that phenol degradation involves both ortho- and meta pathway. The catabolic efficiency of catechol-1,2-dioxygenase and catechol-2,3-dioxygenase was determined by specific enzyme activities. Comparatively higher activity of catechol-1,2-dioxygenase (0.39 U/mg) against that of catechol-2,3-dioxygenase (1.36×10^{-2} U/mg) suggests efficiency of ortho- over meta pathway in diatom BD1IITG. Mahiuddin et al. (2012) reported simultaneous activity of meta- as well as ortho pathway in *Pseudomonas fluorescens* PU1. They reported

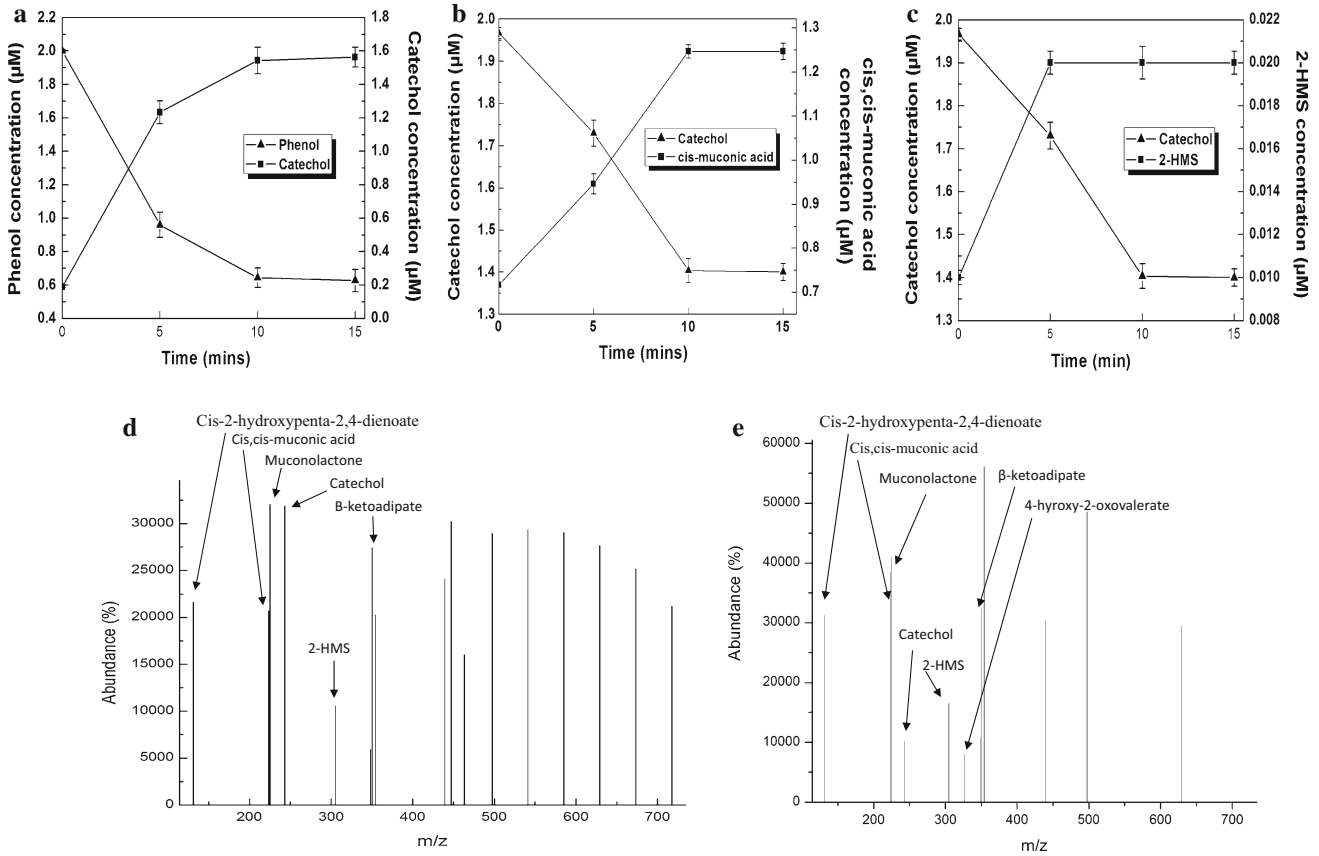

Fig. 5 **a** Phenol hydroxylase activity, **b** catechol-1,2-dioxygenase activity, **c** catechol-2,3-dioxygenase activity, **d** metabolite identification by LC–MS (0 min), **e** metabolite identification by LC–MS (20 min), **f** proposed pathway for phenol degradation in diatom BD1IITG

higher meta activity over ortho activity. Cai et al. (2007) also reported similar findings of coexistence of both ortho- and meta pathway in *Fusarium* species. Semple and Cain (1996) reported meta pathway activity in golden brown chrysophyte alga *Ochromonas danica,* whereas most eukaryotes generally utilize ortho pathway for phenol degradation (Basha et al. 2010). Evidence of ortho activity in other eukaryotes as *Trichosporon cutaneum* (Neujhar and Gaal 1973), *Penicillium* sp. (Hofrichter et al. 1993), *Fusarium* sp., *Aspergillus* sp., *Penicillium* sp. and *Graphium* sp. (Santos and Linardi 2004), *Candida* sp. (Tsai et al. 2005) correlates with the present finding.

The metabolites produced by breakdown of *cis*,*cis*-muconic acid (ortho pathway) and 2-hydroxymuconic semialdehyde (meta pathway) were identified by LC–MS analysis. For metabolite identification, catechol dioxygenase assay mixture both at start and end of the reaction was analyzed and the respective chromatograms have been shown in Fig. 5d, e. The chromatogram at the start of the assay (Fig. 5d) shows a *m*/*z* signal at 243.21 high abundance (abundance = 31,886) consistent with the molecular ion mass of [2 M + Na] adduct of catechol. Other *m*/*z* signals correspond to molecular ion mass adducts of ortho pathway metabolites as *cis*,*cis*-muconic acid (adduct = M + 2ACN + H, *m*/*z* value = 223.16, abundance = 20,721), muconolactone (*m*/*z* value = 225.17, Adduct = M + 2ACN + H, abundance = 32,048) and β-ketoadipate (*m*/*z* value = 348.27, Adduct = 2 M + $3H_2O$ + 2H, abundance = 5944). Similarly, the assay mixture (Fig. 5d) also contained molecular ion mass adducts of meta pathway metabolites as 2-HMS (*m*/*z* value = 305.19, adduct = 2 M + Na, abundance = 10,541) and *cis*-2-hydroxypenta-2,4-dienoate (*m*/*z* value = 131.17, Adduct = M + NH_4, abundance = 21,618).The formation of adduct ions is common occurrence in LC–MS analysis. Adduct ions as sodium adduct [M + Na], ammonium adduct [M + NH_4], adducted solvent molecules as [M + H + H_2O] are routinely observed in positive ion electrospray analysis. Biological samples generally have high endogenous concentration of various salts, while other salts may be added during sample preparation. This justifies the high probability of adduct ion formation during LC–MS of biological samples (Klink 2014). After incubation period of 20 min, in the LC–MS chromatogram of the assay mixture (Fig. 5e) the abundance of the *m*/*z* signal at 243.21 correspond to catechol decrease confirming its

Fig. 5 continued

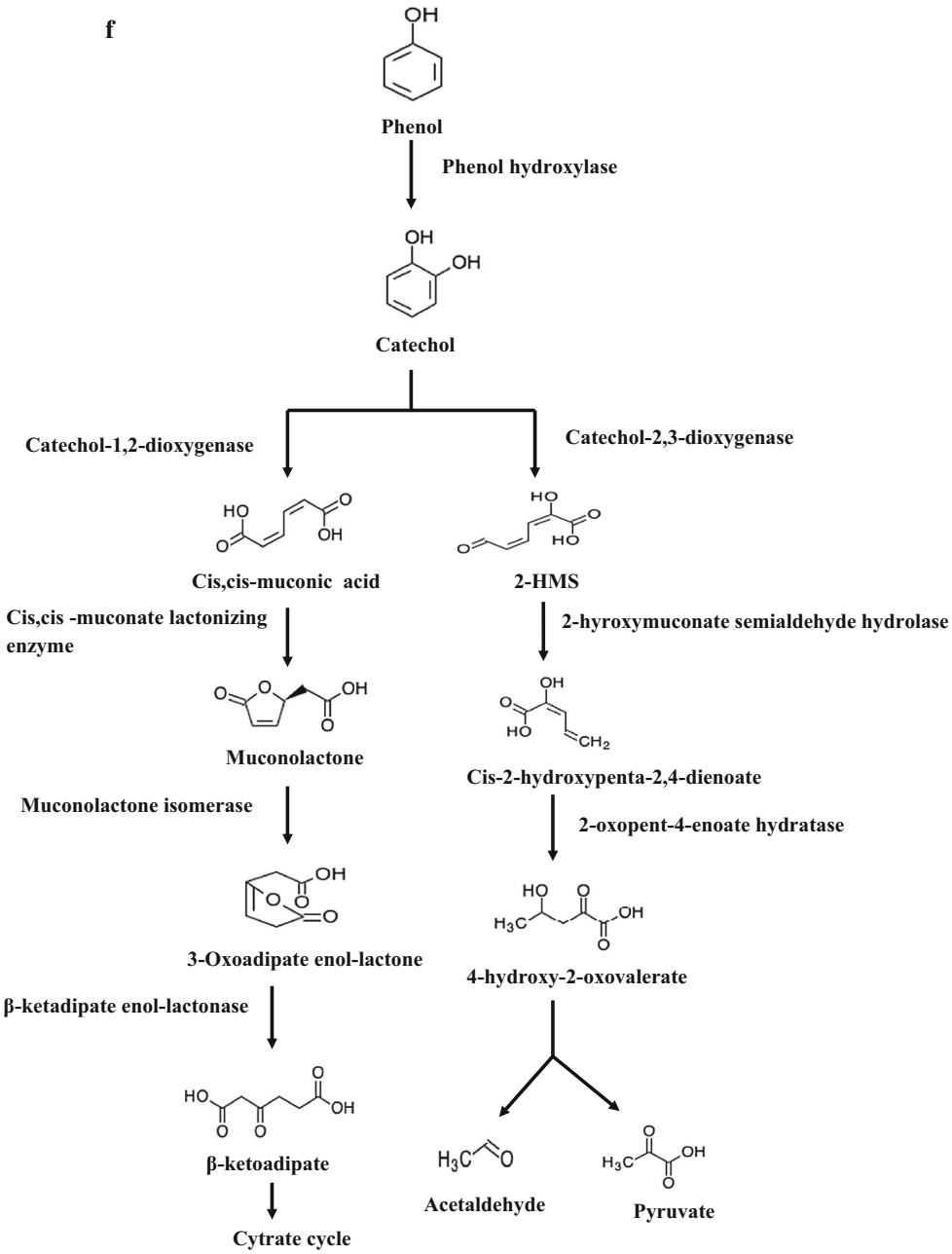

utilization during the assay. The increase in abundance of *m*/*z* signals corresponding to ortho pathway metabolites as *cis*,*cis*-muconic acid (*m*/*z* value = 223.16, abundance = 38,434), muconolactone (*m*/*z* value = 225.17, abundance = 41,054) and β-ketoadipate (*m*/*z* value = 348.27, abundance = 10,794) indicates that catechol is being ortho cleaved by catechol-1,2-dioxygenase to *cis*,*cis*-muconic acid. The identification of products found downstream of *cis*,*cis*-muconic acid in the ortho pathway indicates breakdown of *cis*,*cis*-muconic acid. *Cis*,*cis*-muconic acid is lactonized by *cis*,*cis*-muconate lactonizing enzyme to muconolactone. Muconolactone isomerase catalyzes the isomerization of muconolactone to 3-oxoadipate-enol-lactone (L.N. Ornston,1966). However, *m*/*z* signal corresponding to 3-oxoadipate-enol-lactone was not identified during LC–MS analysis (Fig. 5e) in the present study. Identification of β-ketoadipate, the next metabolite in the pathway formed by hydrolysis of 3-oxoadipate-enol-lactone by β-ketoadipate enol-lactonase, gives an evidence of the existence of oxoadipate-enol-lactone in the phenol degradation pathway. The assay mixture following incubation (Fig. 5e) also showed increased abundance for *m*/*z* signal corresponding to meta pathway metabolites as 2-HMS (*m*/*z* = 305.19, abundance = 16,537), *cis*-2-hydroxypenta-

2,4-dienoate (*m/z* value = 131.17, abundance = 31,213). Another *m/z* signal corresponding to another meta pathway metabolite 4-hydroxy-2-oxovalerate (*m/z* signal = 326.24, adduct = 2 M + ACN + Na, abundance = 8156) could be detected by LC–MS analysis (Fig. 5e). This confirms that catechol-2,3-dioxygenase activity is involved in the meta cleavage of catechol ring to 2-HMS. The identification of products downstream of 2-HMS in meta pathway confirms that the metabolism of 2-HMS. 2-hyroxymuconate semialdehyde hydrolase causes hydrolysis of 2-HMS to *cis*-2-hydroxypenta-2,4-dienoate. 2-oxopent-4-enoate hydratase activity produces 4-hydroxy-2-oxovalerate from *cis*-2-hydroxypenta-2,4-dienoate.

On the basis of enzyme activity studies and metabolite identification, the proposed pathway for phenol degradation in the diatom BD1IITG has been shown in Fig. 5f. The proposed pathway was found to have similarities with algal (Semple and Cain 1996), fungal (Tsai et al. 2005; Cai et al. 2007; Santos and Linardi 2004) as well as bacterial (Mahiuddin et al. 2012; Ali et al. 1998) catabolic mechanisms.

Biosurfactant production

Emulsification assay suggested that diatom BD1IITG released biosurfactant into the medium which facilitated the phenol degradation process (Fig. 6). The extracellular accumulation of the biosurfactant concomitantly with phenol degradation makes the role of biosurfactant in facilitating phenol degradation clearly evident. From Fig. 7, the biosurfactant emulsifying activity is found to be dependent on initial phenol concentration. The highest emulsifying activity has been observed at 100 mg/l phenol (Fig. 6) where the biomass growth as well as phenol degradation rate of diatom BD1IITG was found to be the highest (Fig. 2c). Thus, the phenol degradation process of the diatom BD1IITG is accompanied by the release of biosurfactant in the medium which may improve the biodegradation efficiency as well as lower the toxicity of phenol on the cells (Hassan et al. 2014; Rocha et al. 2007). Similar results of biosurfactant production during the process of phenol degradation have been reported for *Candida tropicalis* (Rocha et al. 2007).

Potential applications of spent biomass

This section verifies the potential of the phenol-degrading biomass to serve as biofuel feedstock. Microalgal biomass with high lipid and polysaccharide content can serve as feedstock for biodiesel and bioethanol, respectively (Gracia et al. 2006; Kong et al. 2013; Kavitha et al. 2014). The desirability of diatoms as a biodiesel feedstock lies in the fact that it contains 25 % lipids/dry weight which is 8 %

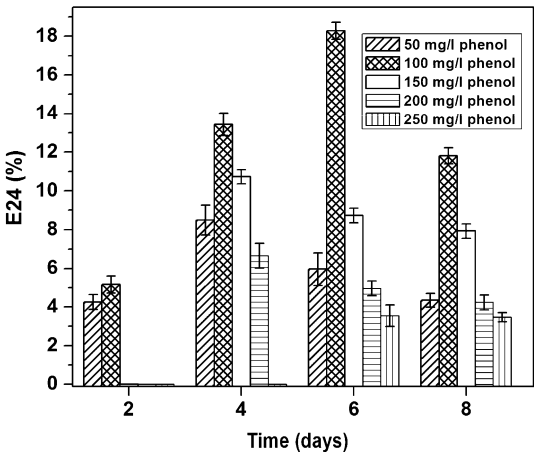

Fig. 6 Emulsification index (E 24) of diatom BD1IITG in phenol-containing culture media

higher than other green algae (Levitan et al. 2014). Diatoms predominantly produce 13–21 carbon chain fatty acids composed mainly of saturated and monosaturated fatty acids (MUFAs) which is necessary to produce biodiesel of optimal quality (Levitan et al. 2014). Moreover, C14 chain length carbon atoms are most highly enriched in diatom as compared to their deficiency in other algal classes (Hidelbrand et al. 2012). The lipid profile of diatom suggests it to be potential target to be utilized as biodiesel feedstock. The biochemical analysis of the diatom BD1IITG biomass was carried out using FTIR in a bid to characterize its potential applicability for biofuel applications. The infrared region 2875–2850 cm^{-1} corresponds to symmetric stretching of CH_2 and CH_3 of lipids. Decreased transmittance in this region in phenol-incubated cells as compared to control cells suggests increased lipid accumulation in phenol-degrading biomass (Fig. 7a). The findings of increased lipid biosynthesis in *Phaeodactylum tricornutum* UTEX-640 (Gracia et al. 2006) and *Chlorella vulgaris* (Kong et al. 2013) when cultured mixotrophically with carbon sources as glycerol, fructose and glucose accord with present finding of increased lipid accumulation in the presence of phenol as additional carbon source. Owing to increased lipid content, the diatom biomass (after phenol biodegradation) could serve as potential raw material for biodiesel production. It is well-reported fact that mixotrophic cultivation allows microalgae to accumulate higher proportion of lipids within less time (Yang et al. 2011). However, its commercial applicability is hindered by high substrate cost. The carbon source accounts for 50 % of the cost of culture medium used in mixotrophic algal cultivation. This makes the process of production of biomass feedstock for biodiesel costly (Yang et al. 2011). Thus, cheap alternative carbon sources for mixotrophic cultivation could help commercialize biodiesel by reducing the cost of production of biomass

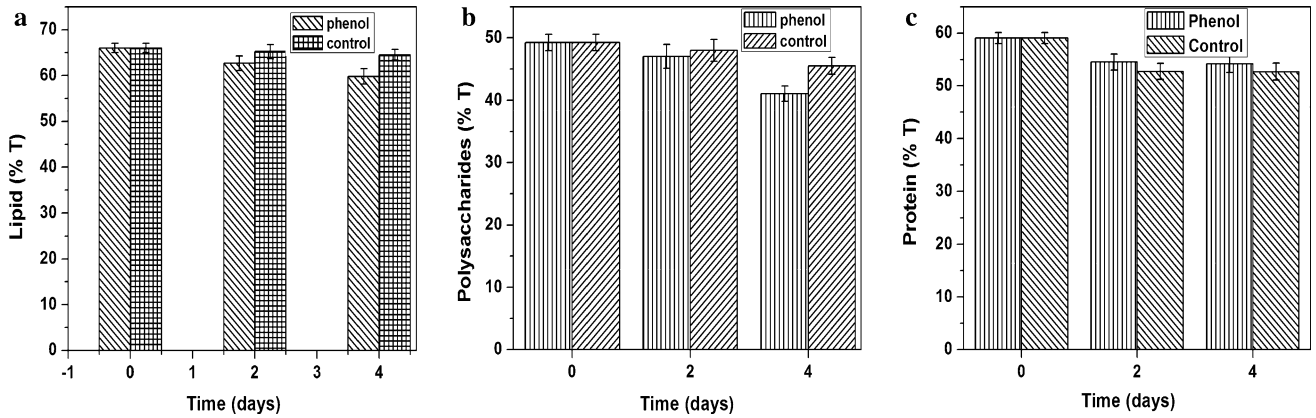

Fig. 7 **a** Change in FTIR peak transmittance corresponding to symmetric stretching of CH_2 and CH_3 of lipids, **b** change in FTIR peak transmittance corresponding to stretching of C–O–C of polysaccharides, **c** change in FTIR peak transmittance corresponding to C=O stretching of proteins

feedstock. The present study shows that diatom BD1IITG has increased lipid biosynthesis (Fig. 7a) while metabolizing phenol which is a waste product of various industrial processes. Thus, mixotrophic cultivation of the diatom BD1IITG using industrial waste phenol as a carbon source could provide exciting possibility to decrease the production cost of biomass feedstock for biodiesel. The infrared region 1200–900 cm^{-1} corresponds to symmetric stretching of C–O–C of polysaccharides (Murdock and Wetzel 2009). The decreased transmittance data in this region indicate increased polysaccharide accumulation in phenol-degrading biomass as compared to control biomass (Fig. 7b). Increased polysaccharide content in phenol-degrading biomass indicates its potential to serve as a bioethanol feedstock (Chaudary et al. 2014). The infrared region 1610–1685 cm^{-1} is associated with C=O stretching of proteins (Murdock and Wetzel 2009). Decreased transmittance in this region indicates increased protein biosynthesis in control biomass in comparison with that in phenol-degrading biomass (Fig. 7c). Owing to increase in biosynthesis of lipids and polysaccharide in the diatom BD1IITG biomass during the phenol degradation process, the spent biomass (after phenol degradation) could be potentially employed for lipid extraction for biodiesel application. The defatted (lipid extracted) biomass could then be utilized for bioethanol production owing to its enhanced polysaccharide content (Kavitha et al. 2014).

Conclusion

A phenol-degrading diatom BD1IITG (GenBank Accession No. KJOO2533) was isolated from petroleum refinery wastewater. The diatom could degrade 39.88 % (for 50 mg/l phenol), 63 % (for 100 mg/l phenol), 59.52 % (for 150 mg/l phenol), 51.23 % (for 200 mg/l phenol) and 24 % (for 250 mg/l phenol). The specific degradation rate was highest at 100 mg/l phenol due to highest specific growth rate at this concentration. Diatom BD1IITG could mineralize 68.58 % of 23.33 mg/l phenol in refinery wastewater. The growth behavior of the diatom in nutrient media as well as refinery wastewater was best represented by Haldane model. Biokinetic parameters of μ_{max} (0.4 day^{-1}), K_I (90.24 mg/l), K_s (20.99 mg/l) obtained by growth kinetic modeling suggest that the diatom possesses higher maximum specific growth rate, better tolerance to toxicity as well as high affinity for phenol in petroleum refinery wastewater. These kinetic parameters suggest the potential for practical applicability of the strain for phenol remediation in petroleum refinery wastewater. Along with phenol (aromatic compound), the diatom could also remove alkanes from refinery wastewater. Cometabolism of alkane along with phenol could provide two parallel carbon sources for the cell leading to enhanced biomass growth and thus increased phenol uptake rates in petroleum refinery wastewater. FTIR analysis shows intracellular phenol uptake and its breakdown into downstream products, suggesting that the phenol removal process in the diatom involves biodegradation and not bioaccumulation. The diatom degrades phenol by both ortho- as well as meta pathway. However, ortho pathway is predominantly active over the meta pathway. During the process of phenol degradation, the diatom produces biosurfactant which may facilitate in increasing the phenol degradation efficiency and lowering the toxicity of phenol on the cells. The highest emulsifying activity of biosurfactant has been observed at 100 mg/l phenol where there is maximum phenol degradation rate. Infrared analysis confirms increased biosynthesis of lipids and polysaccharides in the diatom BD1IITG biomass during the phenol degradation process. Owing to increase in content of lipids and polysaccharides, the spent biomass (after phenol

degradation) could be potentially used lipid extraction for biodiesel application. The defatted (lipid extracted) biomass could then be used as a feedstock for bioethanol production due to its enhanced polysaccharide content. Thus, the process of mixotrophic growth of diatom BD1IITG on phenol could prove to be a clean environmentally sustainable process as: First, the diatom can metabolize phenol as a carbon source thus remediating the toxic effect of phenol on the environment. Secondly, the biomass after phenol degradation could potentially serve as biodiesel and bioethanol feedstock. The utilization of industrial waste and water pollutant phenol as a carbon source for mixotrophic algal culture could provide a cheaper and easily available source of substrate. This could decrease the production cost of biomass feedstock for biodiesel applications thus overcoming a major bottleneck in commercialization of biodiesel. Thus, the paradigm of enhanced lipids and polysaccharides in phenol-degrading diatom biomass deserves adequate attention and is being currently studied in our laboratory.

Acknowledgments Authors acknowledge Indian Institute of Technology for providing research fellowship to pursue doctoral studies at the Centre for the Environment. The present work is not financially supported by any funding agency.

References

Abdelwahab O, Amin NK, El-Ashtoukhy E-SZ (2009) Electrochemical removal of phenol from oil refinery wastewater. J Haz Mat 163:711–716

Agarry SE, Durojaiye AO, Yusuf RO, Aremu MO (2008) Biodegradation of phenol in refinery wastewater by pure cultures of *Pseudomonas aeruginosa* NCIB 950 and *Pseudomonas fluorescence* NCIB 3756. Int J Environ Pollut 32:3–11

Aiba S, Shoda M, Nagatani M (1968) Kinetics of product inhibition in alcohol fermentation. Biotechnol Bioeng 10:845–864

Ali S, Fernandez-Lafuente R, Cowan DA (1998) Meta-pathway degradation of phenolics by thermophilic *Bacilli*. Enz Microb Technol 23:462–468

Banerjee A, Ghoshal AK (2010) Phenol degradation by *Bacillus cereus*: pathway and kinetic modeling. Bioresour Technol 101:5501–5507

Baranyi J (2010) Modelling and parameter estimation of bacterial growth with distributed lag time, Dissertation, University of Szeged

Basha KM, Rajendran A, Thangavelu V (2010) Recent advances in the biodegradation of phenol: a review. Asian J Exp Biol Sci 2:219–234

Cai W, Li J, Zhang Z (2007) The characteristics and mechanisms of phenol biodegradation by *Fusarium* sp. J Hazard Mater 148:38–42

Chaudary L, Pradhan P, Soni N, Singh P, Tiwari A (2014) Algae as feedstock in bioethanol production: new entrance in biofuel world. Int J ChemTechnol Res 2:1381–1389

Deereeper A, Guignon V, Blanc G, Audic S, Buffet S, Chevenet F, Dufayard JF, Guindon S, Lefort V, Lescot M, Gascuel OJM (2008) Phylogeny.fr: robust phylogenetic analysis for the non-specialist. Nucleic Acids Res 36:465–469

Droussi ZD, Rosaria V, Provenzano M, Hafidi M, Ouatmane A (2009) Study of the biodegradation and transformation of olive-mill residues during composting using FTIR spectroscopy and differential scanning calorimetry. J Hazard Mater 164:1281–1285

Duan Z (2011) Microbial degradation of phenol by activated sludge in a batch reactor. Environ Protec Eng 37:53–63

Edwards VH (2004) The influence of high substrate concentrations on microbial kinetics. Biotechnol Bioeng 12:679–712

El Naas MH, Al-Zuhair S, Al Hajja MA (2010) Removal of phenol from petroleum refinery wastewater through absorption on date pit activated carbon. Chem Eng J 162:997–1005

El-Sheekh MM, Ghareib MM, EL-Souod GWA (2012) Biodegradation of phenolic and polycyclic aromatic compounds by some algae and cyanobacteria. J Bioremed Biodegrad 3:133

Firozjaee TT, Najafpour GD, Khavarpour M, Bakhshi Z, Pishgar R, Mousavi N (2011) Phenol biodegradation kinetics in an anaerobic batch reactor. Iran J Environ 2:68–73

Gracia MCC, Camacho GF, Miron AS, Sevilla JMF, Chisti Y, Grima EM (2006) Mixotrophic production of marine microalga *Phaeodactylum tricornutum* on various carbon sources. J Microbiol Biotechnol 16:689–694

Haldane JBS (1965) Enzyme. MIT Press, Cambridge

Hasan SA, Jabeen S (2015) Degradation kinetics and pathway of phenol by *Pseudomonas* and *Bacillus* sp. Biotechnol Biotechnol Equipm 29:45–53

Hassan M, Essam T, Yassin AS, Salama A (2014) Screening of biosurfactant production ability among organic pollutants degrading isolates collected from Egyptian environment. Microb Biochem Technol 6:4

Hidelbrand M, Davis AK, Smith SR, Traller JC, Abbriano R (2012) The place of diatom in the biofuel industry. Biofuels 3:221–240

Hofrichter M, Gunther T, Fritsche W (1993) Metabolism of phenol, chloro and nitrophenol by Penicillium strain Bi 7/2 isolated from a contaminated soil. Biodegradation 3:415–421

Joo HN, Lee CG (2007) Antibiotics addition as an alternative sterilization method for axenic cultures in *Haematococcus pluvialis*. J Ind Eng Chem 13:110–115

Jou CJG, Huang GC (2003) A pilot study for oil refinery wastewater treatment using a fixed-film bioreactor. Adv Environ Res 7:463–469

Kavitha C, Ashokkumar V, Chinnasamy S, Bhaskar S, Rengasamy R (2014) Pretreatment of lipid extracted *Brotryococcus braunii* spent biomass for bioethanol production. Int J Curr Biotechnol 2:11–18

Kelknar V, Kosarnic N (1992) Degradation of phenols by algae. Environ Technol 13:493–501

Klink F (2014) Dealing with metal adduct ions in electrospray. http://www.sepscience.com/Information/Archive/MS-Solutions/233-/MS-Solutions-3-Dealing-with-Metal-Adduct-Ions-in-Electrospray-Part-1. Accessed 11 May 2014

Kong WB, Yang H, CaoYT Song H H, Xia SF (2013) Effect of glycerol and glucose on the enhancement of biomass, lipid and soluble carbohydrate production by *Chlorella vulgaris* in mixotrophic culture. Food Technol Biotechnol 51:62–69

Levitan O, Dinamarca J, Hochman G, Falkowski PG (2014) Diatoms: a fossil fuel of the future. Trends Biotechnol 32:117–124

Li Y, Li J, Wang C, Wang P (2010) Growth kinetics and phenol biodegradation of psychrotrophic *Pseudomonas putida* LY1. Bioresour Technol 101:6740–6744

Lovell CR, Eriksen NT, Lewitus AJ, Chen YP (2002) Resistance of the marine diatom *Thalassiosira* sp. to toxicity of phenolic compounds. Mar Ecol Progr 229:11–18

Mahiuddin MD, Fakhruddin ANM, Al-Mahin A (2012) Degradation of phenol via meta cleavage pathway by *Pseudomonas fluorescens* PU1. ISRN Microbiol 12:1–6

Mathur AK, Majumder CB (2010) Kinetics modelling of the biodegradation of benzene, toluene and phenol as single substrate and mixed substrate by using *Pseudomonas putida*. Chem Biochem Eng 24:101–109

Murdock JN, Wetzel DL (2009) FTIR microspectroscopy enhances biological and ecological analysis of algae. Appl Spectroscop Rev 44:335–361

Neujhar HY, Gaal A (1973) Phenol hydroxylase from yeast. Eur J Biochem 35:386–400

Ojumu TV, Bello OO, Sonibare JA, Solomon BO (2005) Evaluation of microbial systems for bioremediation of petroleum refinery effluents in Nigeria. Afr J Biotechnol 4:31–35

Ornston LN (1966) The conversion of catechol and protocatechuate to β-ketoadipate by *Pseudomonas putida*: III enzymes of the catechol pathway. J Biol Chem 241:3800–3810

Páca J Jr, Kremláčková V, Turek M, Suchá V, Vilímková L, Páca J, Halecký M, Stiborová M (2007) Isolation and partial characterization of cytoplasmic NADPH-dependent phenol hydroxylase oxidizing phenol to catechol in Candida tropicalis yeast. Enz Microb Technol 40:919–926

Pinto G, Pollio A, Previtera L, Stanzione M, Temussi F (2003) Removal of low molecular weight phenols from olive oil mill wastewater using microalgae. Biotechnol Lett 25:1657–1659

Rocha LL, Cordeiro RDA, Cavalcante RM, Nascimento RFD, Martins SCS, Santaella ST, Melo VMM (2007) Isolation and characterization of phenol degrading yeasts from an oil refinery wastewater in Brazil. Mycopathol 164:183–188

Sahoo NK, Ghosh PK, Pakshirajan K (2011) Kinetics of 4-bromophenol degradation using calcium alginate immobilized *Arthrobacter chlorophenolicus A6*. Int J Earth Sci Eng 4:663–668

Santos VL, Linardi VR (2004) Biodegradation of phenol by a filamentous fungi isolated from industrial effluents—identification and degradation potential. Process Biochem 39:1001–1006

Saravanan P, Pakshirajan K, Saha P (2008) Growth kinetics of an indigenous mixed microbial constrotium during phenol degradation in a batch reactor. Bioresour Technol 99:205–209

Scragg AH (2006) The effect of phenol on the growth of *Chlorella vulgaris* and Chlorella VT-1. Enzym Microb Technol 39:796–799

Semple KT, Cain RB (1996) Biodegradation of phenol by algae Ochromonas danica. Appl Environ Microbiol 62:1265–1273

Senthivelan T, Kanagaraj J, Panda RC, Mandal AB (2014) Biodegradation of phenol by mixed microbial culture: an ecofriendly approach for pollution reduction. Clean Technol Environ Policy 16:113–126

Sun JQ, Xu L, Tang YQ, Chen FM, Wu XL (2012) Simultaneous degradation of phenol and n-hexadecane by *Acinetobacter* strains. Bioreour Technol 123:664–668

Tsai SC, Tsai LD, Li YK (2005) An isolated *Candida albicans* TL3 capable of degrading phenol at large concentration. Biosci Biotechnol Biochem 69:2358–2367

Webb JL (1963) Enzyme and metabolic inhibitors. Academic Press, USA

Wharfe ES, Jarvis RM, Winder CL, Whiteley AS, Goodacre R (2010) Fourier transform infrared spectroscopy as a metabolite fingerprinting tool for monitoring the phenotypic changes in complex bacterial communities capable of degrading phenol. Environ Microbiol 12:3253–3263

Yang JS, Rasa E, Tantayotai P, Scow KM, Yuan HL, Hristova KR (2011) Mathematical model of *Chlorella minutissima* UTEX2341 growth and lipid production under photo-heterotrophic fermentation conditions. Bioresour Technol 102:3077–3082

Yano T, Nakahara T, Kamiyama S, Yamada K (1966) Kinetic studies on microbial activities in concentrated solutions I Effect of excess sugars on oxygen uptake rate of a cell free respiratory system. Agric Biol Chem 30:42–48

Zhao X, Wang Y, Ye Z, Borthwick AGL, Ni J (2006) Oil field wastewater treatment in Biological Aerated Filter by immobilized microorganisms. Process Biochem 41:1475–1483